Millimeter Wave I-Q Standoff Biosensor

Shaolin Liao[*a], Sasan Bakhtiari[a], Thomas Elmer[a], Apostolos C. Raptis[a]
Ilya V. Mikhelson[b], and Alan V. Sahakian[b]
[a]Argonne National Laboratory, Lemont, IL, USA 60439;
[b] Dept. of Electrical Engr. and Computer Sci., Northwestern University, Evanston, IL, USA 60208

ABSTRACT

A continuous wave (CW) 94-GHz millimeter wave (mmW) standoff biosensor has been developed for remote biometric sensing applications. The sensor measures the demodulated in-phase (I) and quadrature-phase (Q) components of the received reflected mmW signal from a subject. Both amplitude and phase of the reflected signal are obtained from down-converted I and Q channels from the quadrature mixer. The mmW sensor can faithfully monitor human vital signs (heartbeat and respiration) at relatively long standoff distances. Principle Component Analysis (PCA) is used to extract the heartbeat, the respiration and the body motion signals. The approach allows one to deduce information about amplitude and beat-to-beat rate of the respiration and the heartbeat. Experimental results collected from a subject were analyzed and compared to the signal obtained with a three-electrode ECG monitoring instrument.

Keywords: CW, millimeter wave, quadrature mixer, PCA, ECG

1. INTRODUCTION

Remote diagnostics of biometric signatures of living humans are critical for both civil and homeland security applications [1-2]. Compared to conventional methods that employ electrical or mechanical sensors, e.g., ECG, which requires direct attachment of electrodes to the subject [3-4], standoff measurement techniques do not require contact with the subject. This criterion is of utmost importance in cases like severe burns or for monitoring of patients after a disaster. Recently, there has been a dramatic growth of interest in remote sensing of physiological signals like respiration and heartbeat using microwave and millimeter waves at different frequencies such as 2.4 GHz [5], 10 GHz [6], and 60 GHz [7]. The main criteria for the choice of frequency are the spatial resolution, the measurement range and the effect of ambient conditions. In addition to difference among the hardware implementation methods, different signal processing methods have also been used to extract the respiration and heartbeat signatures from the complicated reflected signals, e.g., spectrogram based on time segment Fourier Transform (FT), wavelet transform and parameter fitting used by the authors [1]. Here, we show the results of our investigations using a 94-GHz mmW I-Q sensor for remote monitoring of biometric signals. We show that heartbeat, respiration and body motion signals can be faithfully extracted using the powerful Principal Component Analysis (PCA) method. This paper is organized as follows: Section 2 describes the architecture of our 94-GHz mmW biosensor. Section 3 presents the theoretical background of the PCA method. Section 4 shows the experimental results and PCA extraction. Finally, some concluding remarks are presented in Section 5.

2. 94-GHZ MMW STANDOFF I-Q BIOSENSOR

2.1 Sensor architecture

Our 94-GHz mmW sensor is based on the I-Q demodulation technique, which extracts both amplitude and phase information from I and Q channels simultaneously. The measurement setup and block diagram of the sensor is shown in Fig. 1. The 94-GHz signal is generated by a Gunn Oscillator, which is then passed through a circulator to a Gaussian lens antenna, which focuses the beam at a region of interest on a subject located at the far field. The reflected signal from the target is collected by the same Gaussian lens antenna and circulated to the RF port of an I-Q demodulator. A fraction of the Gunn oscillator output is directed to the Local Oscillator (LO) port of the demodulator.

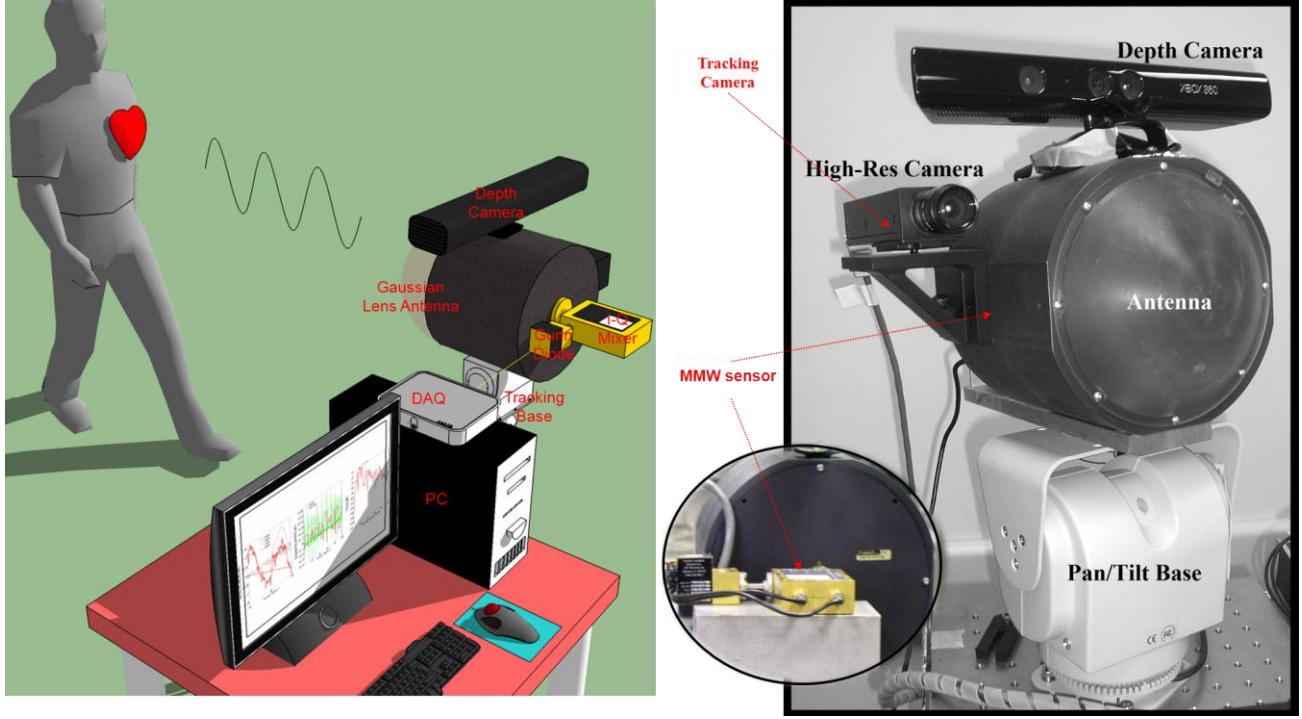*sliao@anl.gov; phone 1 630 252-9204; fax 1 630 252-3250; anl.gov

Figure 1. Measurement scheme and block diagram of the 94-GHz mmW sensor (see text for explanation).

A tracking camera is used to accurately focus the mmW beam spot on the desired area of the target. A program running on a personal computer provides a user friendly interface for collecting I and Q signals via the Data Acquisition (DAQ) board.

2.2 Fundamental principle

The underlying principle of the mmW I-Q sensor is similar to Doppler radar, where motion of subject causes frequency shift $\delta f(t)$ from the carrier frequency f ,

$$\delta f(t) = \frac{v(t)}{c} f \tag{1}$$

where v is the subject velocity and c is the speed of light. The shift of the frequency can be readily obtained through the detection of the phase $\phi_r(t)$ of the reflected signal $r(t)$ for a time-dependent displacement $d(t)$,

$$r(t) = \cos[2\pi f t - \phi_r(t)] = \cos\left[2\pi f t - \frac{4\pi}{\lambda} d(t)\right]$$

$$\delta f(t) = \frac{d\phi_r(t)}{dt} \tag{2}$$

where λ is the carrier wavelength while taking into account the fact that the wave travels twice along the path of the subject's displacement, i.e., forward and backward paths in Eq. (2). In our I-Q sensor, the frequency shift $\delta f(t)$ and phase shift $\phi_r(t)$ are obtained through I-channel data $I(t)$ and Q-channel data $Q(t)$ from the following relations,

$$I(t) = A_r(t)\cos\left[\frac{2\pi}{\lambda} d(t)\right]$$

$$Q(t) = A_r(t)\sin\left[\frac{2\pi}{\lambda} d(t)\right]$$

$$\phi_r(t) = \arctan\left(\frac{I(t)}{Q(t)}\right)$$

$$\mathscr{f}(t) = \frac{[Q(t)]^2}{[I(t)]^2 + [Q(t)]^2}\left[\frac{dI(t)}{dt} - \frac{I(t)}{[Q(t)]^2}\frac{dQ(t)}{dt}\right] \tag{3}$$

Using Eqs. (1) through (3), we obtain the displacement $d(t)$ and velocity $v(t)$ of the subject given by

$$d(t) = \frac{\lambda}{4\pi}\arctan\left(\frac{I(t)}{Q(t)}\right)$$

$$v(t) = \lambda\frac{[Q(t)]^2}{[I(t)]^2 + [Q(t)]^2}\left[\frac{dI(t)}{dt} - \frac{I(t)}{[Q(t)]^2}\frac{dQ(t)}{dt}\right] \tag{4}$$

2.3 I-Q chart

One can obtain the relation between I channel $I(t)$ and Q channel $Q(t)$ as follows,

$$\frac{[I(t)]^2}{[A(t)]^2} + \frac{[Q(t)]^2}{[A(t)]^2} = 1 \tag{5}$$

which means that for an ideal I-Q sensor, the I-Q chart traces circle segments with amplitude $A(t)$ as their radius. However, in the real situation, there is always some deviation from the ideal circle due to unavoidable amplitude ΔA and phase $\Delta\phi$ imbalances of the I-Q sensor,

$$\tilde{I}(t) = A(t)\cos\left[\frac{2\pi}{\lambda}d(t)\right]$$

$$\tilde{Q}(t) = [A(t) + \Delta A]\sin\left[\frac{2\pi}{\lambda}d(t) + \Delta\phi\right] \tag{6}$$

from which the I-Q chart becomes an ellipse if $\Delta\phi = 0$. Since both amplitude ΔA and phase $\Delta\phi$ imbalances are constant values, one can calibrate their values to obtain the corrected $I(t)$ and $Q(t)$. In addition to the mixer imbalance problem, the reflected signal also contains background or stray fields that introduces offsets to both the I and the Q channels, resulting in

$$\tilde{I}(t) = A(t)\cos\left[\frac{2\pi}{\lambda}d(t)\right] + \Delta I$$

$$\tilde{Q}(t) = [A(t) + \Delta A]\sin\left[\frac{2\pi}{\lambda}d(t) + \Delta\phi\right] + \Delta Q \tag{7}$$

As an example, Fig. 2 shows the I-Q chart for 10% amplitude imbalance (unit amplitude here), 10° phase imbalance, at offsets of $\Delta I = 0.5$ and $\Delta Q = 1$. Also shown is an ideal I-Q chart without any imbalance and offset (i.e., a circle).
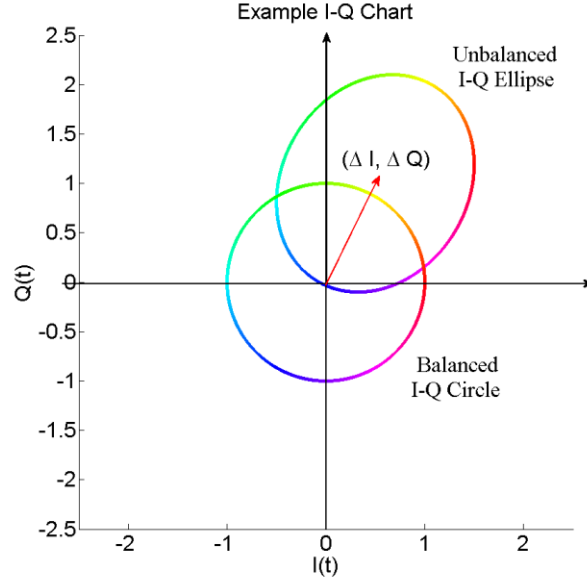
Figure 2. An example of a realistic I-Q chart together with an ideal I-Q chart.

3. PRINCIPAL COMPONENT ANALYSIS (PCA)

The extraction of respiration and heartbeat signal from the reflected signal is nontrivial considering the imbalances and offsets given by Eq. (7). What makes things more complicated is the inevitable body movement, which further corrupts the respiration and heartbeat signals contained in the reflected phase $\phi(t)$. Since the body movement is time-dependent, the global method such as spectrogram based on Fourier Transform (FT) may not allow accurate extraction of the respiration and heartbeat signals. For such situations, Principle Component Analysis (PCA) can be used to simultaneously extract the respiration, heartbeat and body motion signals [8]. To explain the method, let's expand the time-dependent phase $\phi(t)$ as the sum of the heartbeat signal $h(t)$, the respiration signal $r(t)$ and the background signal $b(t)$ (e.g., body motion and baseline etc.),

$$\phi(t) = h(t) + r(t) + b(t) \tag{8}$$

PCA exploits the orthogonal basis of the covariance matrix $\overline{\overline{C}}$ of the Doppler phase signal $\varphi(t)$,

$$\overline{\overline{C}} = \overline{\varphi(t)}^T \overline{\varphi(t)} \tag{9}$$

The eigen-vectors matrix $\overline{\overline{V}}$ of the covariance matrix $\overline{\overline{C}}$ forms an orthogonal basis function, which can be readily computed by decomposing $\overline{\overline{C}}$ in terms of eigen-values $\overline{\overline{E}}$ and eigen-vectors $\overline{\overline{V}}$,

$$\overline{\overline{C}} = \overline{\overline{E}}\,\overline{\overline{V}} \tag{10}$$

Different eigen-vectors represent different time scales and by selection of combinations of different eigen-vectors, e.g., eigen-vectors from $\overline{\overline{V}}(:,I_1)$ to $\overline{\overline{V}}(:,I_2)$, one can obtain the different biometrics patterns such as the heartbeat $H(t)$, the respiration $R(t)$, and the body motion $B(t)$ as,

$$H(t)/R(t)/B(t) = \sum_{i=I_1}^{I_2} \overline{\varphi(t)}^T \overline{\overline{V}}(:,i) \bullet \overline{\overline{V}}(:,i) \tag{11}$$

4. EXPERIMENTAL RESULTS

To evaluate the performance of the I-Q mmW sensor, we have taken two independent data sets for a human subject sitting 2 m away from the sensor with the person 1) holding his breath; and 2) breathing normally. In both experiments, ECG signals were also recorded simultaneously for verification purposes.

4.1 Experimental Data

Figure 3 shows the I-Q chart (right), the ECG signal (top left), the measured phase $\phi(t)$ (middle left) and the amplitude $A(t)$ (bottom left) of the reflected signal for experiment #1, a subject holding his breath. Also, Figure 4 shows the results for experiment #2, subject breathing normally. In both cases, one can clearly see that the phase and amplitude components of the heartbeat $h(t)$ have a much shorter time scale (dips with ~1 second period) compared to those of the respiration $r(t)$ (cosine trend with ~7 second period) and body motion $b(t)$ (slowly varying and non-periodic).
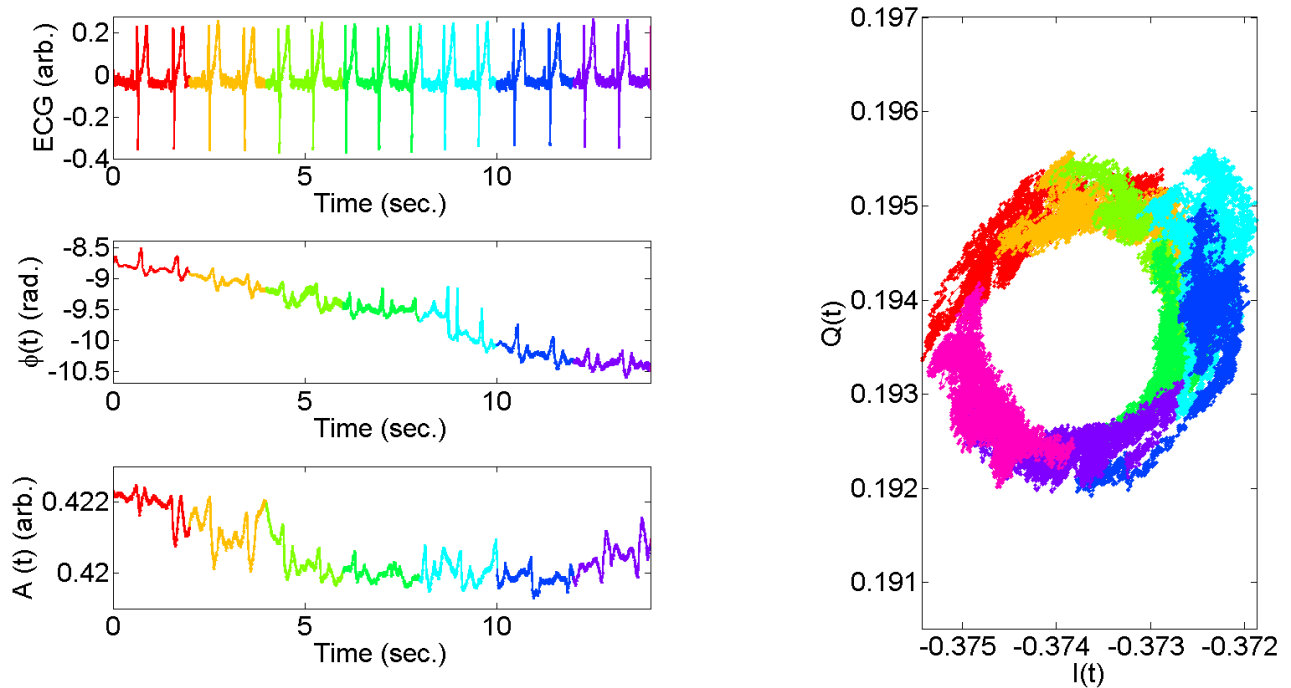

Figure 3. Experiment #1: human subject holding his breath. Shown above are (left) from top to bottom ECG, phase and amplitude of the reflected mmW signals respectively and (right) I-Q chart.
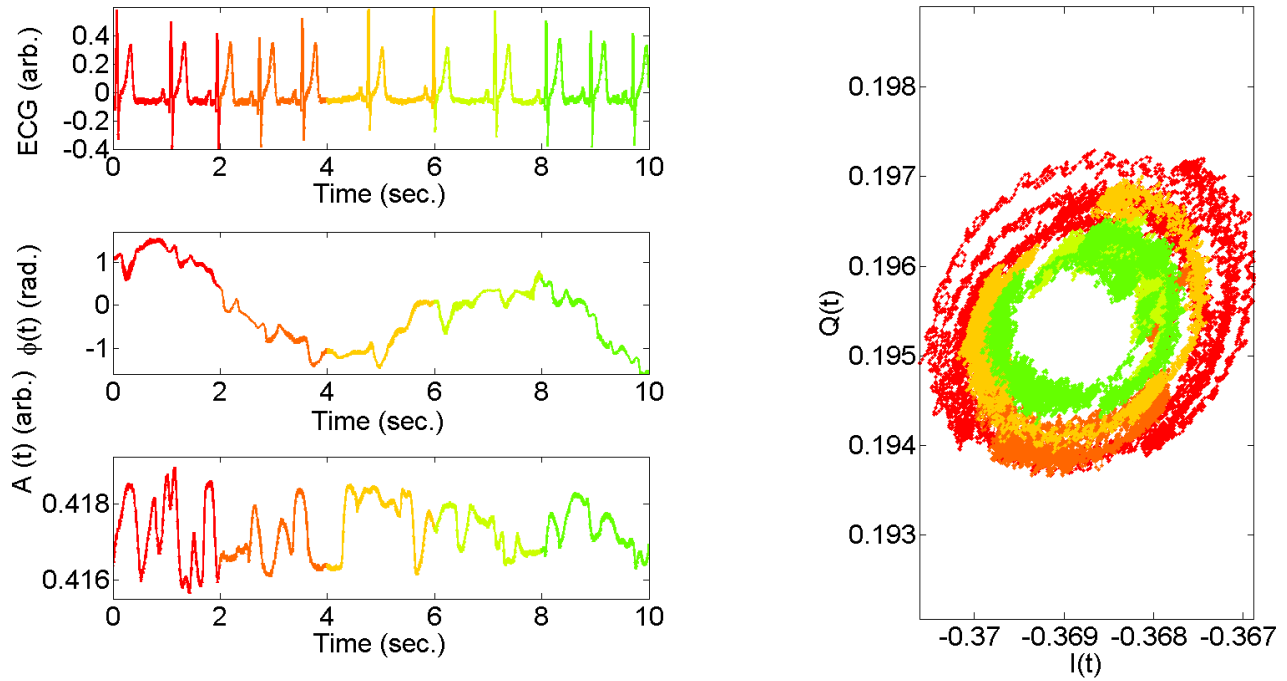
Figure 4. Experiment #2: human subject breathing normally. Shown above are (left) from top to bottom ECG, phase and amplitude of the reflected mmW signal respectively, and (right) I-Q chart.

4.2 PCA

Heartbeat $h(t)$, respiration $r(t)$ and body motion $b(t)$ can be extracted from the data collected in both experiments shown in Figs. 3 and 4, in accordance with the formulation provided in Section 3. Figure 5 shows the PCA extraction results for Experiment #1 when the human subject is holding breath: the extracted heartbeat $h(t)$ agrees well with the ECG signal (center plot in Figure 5) with its Fourier transform showing a mean HR of 1.14 Hz. Similarly, Fig. 6 shows the PCA extraction results for Experiment #2 when the human subject is allowed to breathe normally. Again, the extracted heartbeat $h(t)$ agrees well with the ECG signal (center plot in Figure 6) with its Fourier transform showing a mean HR of 0.9 Hz.
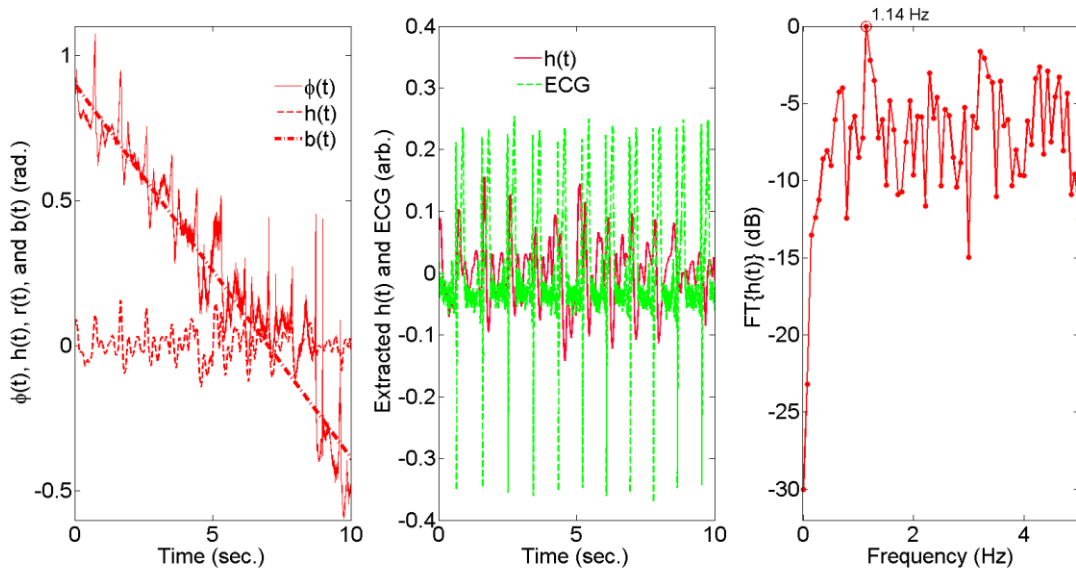
Figure 5. PCA signal analysis for Experiment #1 showing (left) the total phase signal $\phi(t)$, the extracted heartbeat $h(t)$, and the body motion $b(t)$. (middle) agreement between the extracted heartbeat $h(t)$ and the ECG signal, and (right) Fourier transform of the extracted heartbeat $h(t)$ in left and center plots with a mean HR = 1.14 Hz.
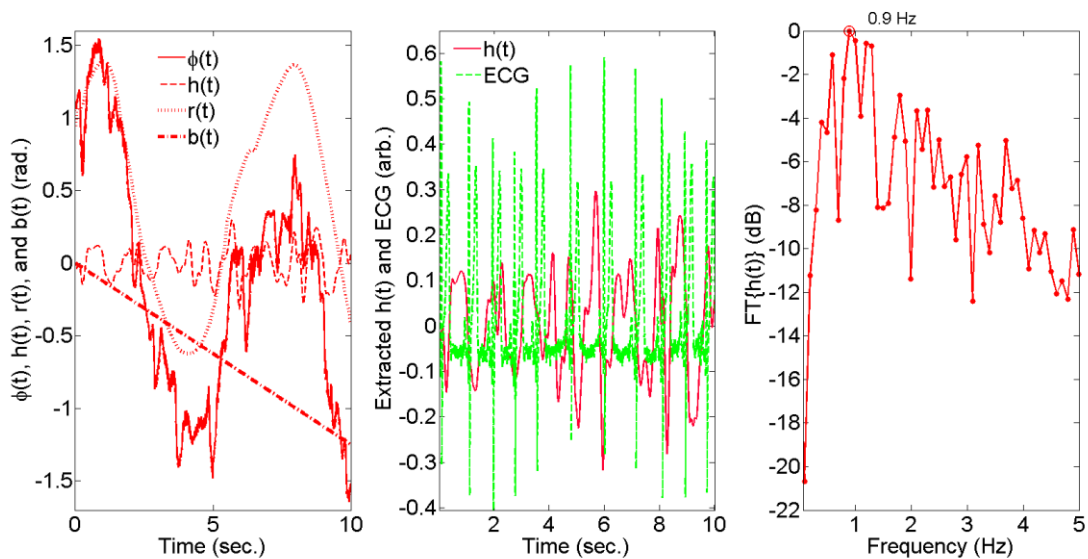

Figure 6. PCA signal analysis for Experiment #2 showing (left) the total phase signal $\phi(t)$, the extracted heartbeat $h(t)$, the respiration $r(t)$ and the body motion $b(t)$. (middle) agreement between the extracted heartbeat $h(t)$ and the ECG signal, and (right) Fourier transform of the extracted heartbeat $h(t)$ in left and middle plots with a mean HR = 0.9 Hz.

5. CONCLUSION

We have developed a 94-GHz mmW standoff biosensor in application to remote measurement of vital signs. The biosensor operates based on the Doppler principle using a quadrature mixer to demodulate the reflected mmW signal. A powerful signal processing method based on PCA has been used to extract heartbeat, respiration and body motion from the measured signals. Two experiment datasets were collected using the biosensor and analyzed using the PCA. The experiments were conducted with the human subject once holding his breath and once breathing normally. The PCA extraction results have shown excellent agreement with the ECG signal that was recorded simultaneously. The results clearly demonstrate the ability of the method to faithfully reveal the vital signs signals such as the beat-to-beat HR, the mean HR, and the respiration rate.

REFERENCES

[1] Bakhtiari, S., Liao, S., Elmer, T. W., Gopalsami, N., and Raptis, A. C., "A Real-Time Heart Rate Analysis for a Remote Millimeter Wave I-Q Sensor," *IEEE Trans. On Biomedical Engineering*, Vol. 58, pp. 1839-1845 (2011).

[2] Mikhelson, I. V., Bakhtiari, S., Elmer, T. W., Sahakian, A. V., "Remote Sensing of Heart Rate and Patterns of Respiration on a Stationary Subject Using 94-GHz Millimeter-Wave Interferometry," *IEEE Transactions on Biomedical Engineering*, Vol. 58, No. 6, pp.1671-1677, June (2011).

[3] J. Fraden and M. R. Neuman, "QRS wave detection," *Med Biol. Eng. Comput.*, vol. 18, pp. 125–132, 1980.

[4] I. K. Daskalov, I. A. Dotsinsk, and I. I. Christov, "Developments in ECG acquisition, preprocessing, parameter measurement and recording," *IEEE Eng. Med. Biol. Mag.*, Vol. 17, No. 2, pp. 50–58, Mar./Apr. 1998.

[5] D. R. Morgan and M. G. Zierdt, "Novel signal processing techniques for Doppler radar cardiopulmonary sensing," *Signal Process.*, Vol. 89, pp. 45–66, 2009.

[6] O. Boric-Lubecke, P. W. Ong, and V. M. Lubecke, "10 GHz Doppler sensing of respiration and heart movement," *in Proc. IEEE 28th Annu. Northeast Bioeng. Conf.*, Philadelphia, PA, Apr. 2002, pp. 55–56.

[7] D. Obeid, S. Sadek, G. Zaharia, and G. El-Zein, "Non-contact heartbeat detection at 2.4, 5.8 and 60 GHz: A comparative study," *Microw. Opt. Technol. Lett.*, Vol. 51, No. 3, pp. 666–669, Mar. 2009.

[8] A. Ferrero, J. Campos, A. M. Rabal, A. Pons, M. L. Hernanz, and A. Corrons, "Principal components analysis on the spectral bidirectional reflectance distribution function of ceramic colour standards," *Optics Express*, Vol. 19, No. 20, 2011.